

# Fluorescence Yields and Molecular Orientation of Thin Organic Films: Vapor-Deposited Oligothiophenes $\alpha 3T$ – $\alpha 8T$

D. Oelkrug,<sup>1</sup> H.-J. Egelhaaf,<sup>1</sup> D. R. Worrall,<sup>2</sup> and F. Wilkinson<sup>2</sup>

---

The fluorescence quantum yields of vapor-deposited (VD) films of  $\alpha$ -oligothiophenes,  $nT$ , with ring numbers of  $n = 3$ – $8$  and layer thicknesses of  $d = 3$ – $50$  nm were determined at room temperature and  $T = 77$  K and compared to the yields of dilute solutions and small  $(5T)_x$  clusters. The yields of highly oriented ultrathin films are of the order of  $\Phi_F = 5 \times 10^{-5}$ – $1 \times 10^{-4}$ . The yields increase strongly with the layer thickness and also upon cooling, but do not reach the values in dilute solution. The main nonradiative deactivation step  $S_1 \rightarrow T_1$  in solution was quantified by  $^1O_2$  production, the yields of which systematically decrease with  $n$  from  $\Phi_\Delta = 0.78$  (3T) to 0.36 (6T), in contrast to the fluorescence yields, which increase from  $\Phi_F = 0.01$  (2T) to 0.40 (6T). In films or clusters the  $S_1 \rightarrow T_1$  deactivation step must be a very unimportant side reaction: neither  $^1O_2$  nor any signal of triplet–triplet absorption could be positively identified.

---

**KEY WORDS:** Thin organic films; vapor-deposited oligothiophenes; quantum yields.

## INTRODUCTION

The excited-state properties of thin organic films are of fundamental importance for possible future applications of these materials as semiconductors, photoconductors or electroluminescent devices. Main candidates of present research are poly- $\pi$ -conjugated hydrocarbons and heterocycles containing, e.g., vinylenes, aromatic rings, or five-membered heterocyclic rings like furan, pyrrol, and thiophene as basic elements for electron transport. The photophysical properties of the single molecular units are usually well understood. However, comparatively little is known about the electronic deactivation pathways when the units are linked together to long chains and subsequently these chains condense to a solid phase.

In the following we investigate the fluorescence yields and some nonradiative deactivation processes in vapor-deposited (VD) thin films and dispersed aggregates of the first members ( $n = 2$  through 8) of the oligothiophenes  $nT$ . The absorption spectra, fluorescence properties, and other deactivation channels of the dissolved molecules up to  $n = 6$  have already been studied [1–15] (7T and 8T are almost insoluble). Also, the absorption [14,16–20] and fluorescence [14,19,21–23] spectra of some oligomers in condensed films are known, including a proposed assignment of the fluorescent state in 6T [21]. It has been shown that  $nT$  films are electroluminescent but the luminescence yield is extremely low in the present stage of device development [24]. In principle, it should be possible to increase the yield by optimizing the molecular arrangement in the film. How to achieve this can be learned from, e.g., the yields of photoluminescence and their dependence on the nature of the film constituting units, the deposition rate, the nature and temperature of the substrate, the film thickness, etc. The oligothiophene films react sensitively on each of these parameters, and we know from the ex-

<sup>1</sup> Institute of Physical and Theoretical Chemistry, University of Tübingen, Tübingen, Germany.

<sup>2</sup> Department of Chemistry, Loughborough University of Technology, Loughborough, UK.

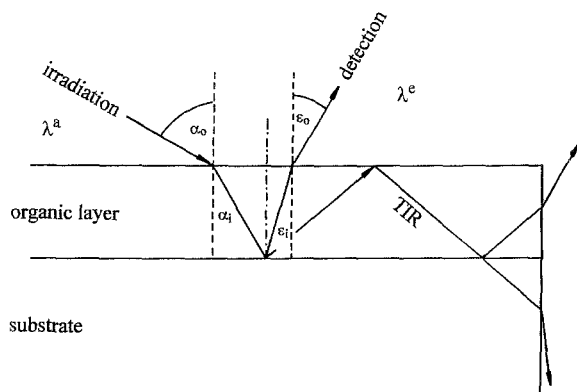


Fig. 1. Geometry for quantitative fluorescence analysis of thin films on transparent or nontransparent substrates (film and substrate thickness not to scale).

treme dichroism of the angular resolved polarized absorption spectra [13,16,25] that this sensitivity originates to a large extent from the tendency of the oligothiophenes to selforganize on polar substrates.

#### DETERMINATION OF FLUORESCENCE YIELDS IN THIN FILMS

The preparation of the  $nT$  layers and the spectroscopic equipment have already been described [13,25]. The layers are strongly dichroic and their absorption and fluorescence emission spectra are therefore measured under variable angles of irradiation ( $\alpha_0$ ) and detection ( $\epsilon_0$ ) (see Fig. 1), as well as under parallel and perpendicular polarization with respect to the plane defined by the directions of incidence and observation. This plane also includes the normal of the sample surface. Calculations of the fluorescence yields need the absorbed fraction of incident light  $A$  and the fluorescence intensity integrated over the whole solid angle. In ultrathin layers the absorbed fraction of light is very small and the transmittance spectra  $T(\lambda^a, \alpha_0)$  have to be properly corrected for reflectance  $R(\lambda^a, \alpha_0)$ , determined in a specular reflectance attachment to the UV/VIS spectrometer,

$$A(\lambda^a, \alpha_0) = [1 - T(\lambda^a, \alpha_0) - R(\lambda^a, \alpha_0)] \quad (1)$$

It turned out that a constant  $R$  value, determined outside the absorption region of the film, was sufficiently accurate in most cases to be inserted in Eq. (1). This approximation was justified by comparing the corrected transmittance with the fluorescence excitation spectra

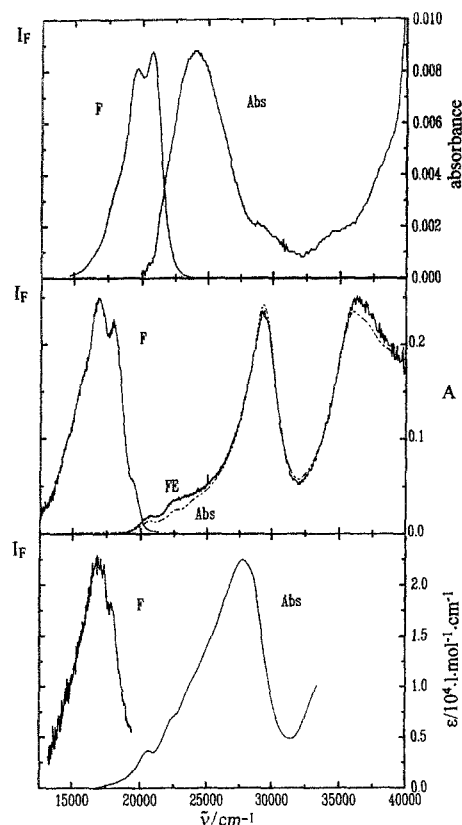


Fig. 2. Absorption (Abs), fluorescence emission (F), and fluorescence excitation (FE) spectra of 5T in different environments. Top: Dilute solution,  $c = 10^{-5} M$ , in a PMMA film of  $d = 4 \mu m$ . Middle: VD film,  $d = 11 nm$ , on fused silica; all spectra are recorded under  $\alpha_0 = 60^\circ$ . The absorption is scaled to  $A = 1 - T - R$ ; the excitation is normalized to the  ${}^1B_u$  absorption maximum. Bottom:  $(5T)_2$  clusters,  $c = 2 \times 10^{-5} M$ , in dioxane/water, 1:1. Concentration and molar extinction coefficient refer to the mass of one 5T unit.

$F(\lambda^a, \alpha_0)$  that are directly proportional to the absorbed part of the incident light

$$F(\lambda^a, \alpha_0) \propto A(\lambda^a, \alpha_0) \quad (2)$$

An example is given in Fig. 2 (middle).

The fluorescence intensities could not be determined satisfactorily up to now by integration over the solid angle. The reason is that most of the fluorescence is guided by total internal reflection (TIR) to the end faces of the layer. We use therefore, as usual, the relative method and compare the unknown material with a reference sample under equal geometric conditions, i.e., equal  $\alpha_0$  and  $\epsilon_0$ , equal (or similar) layer thickness, and equal (or similar) absorbance. The reference sample was a spin-coated layer of 5T in PMMA,  $c = 1 \times 10^{-5} M$ ,  $d = 4 \mu m$ , with  $\Phi_f = 0.32$  (determined under macroscopic

**Table I.** Fluorescence Quantum Yield and Molecular Orientation

System	T2	T3	T4	T5	T6	T7	T8
Diluted solution							
In dioxane, $c < 10^{-5} M$	0.01	0.07	0.18	0.32	0.40		Insoluble
Ultrathin films							
On fused silica and silicon	Not stable in HV		$7 \cdot 10^{-3}$	$5 \cdot 10^{-5}$	$1 \cdot 10^{-4}$	$1 \cdot 10^{-4}$	$1 \cdot 10^{-4}$
Nominal thickness, 3–5 nm	Crystalline islands		Highly oriented with long molecular axes in parallel to the normal of the substrate surface				
Thin films							
Nominal thickness, 20–50 nm	Not stable in HV		$2 \cdot 10^{-2}$	$1.3 \cdot 10^{-3}$	$1.8 \cdot 10^{-3}$	$2 \cdot 10^{-3}$	$1 \cdot 10^{-3}$
			Polycrystalline films; no preferential orientation with respect to the substrate				
Small clusters (T $n$ ) $x$ , $x = 5$ – $10$				$2 \cdot 10^{-3}$			
In dioxane/water, 1:1, $c = 10^{-5} M$							

conditions), whose absorption and fluorescence spectra are shown in Fig. 2 (top). The 5T molecules are isotropically oriented in PMMA and completely fixed during the lifetime of the excited state ( $\tau = 0.9$  ns). Under this condition the fluorescence intensity is angularly distributed according to (provided the emitting transition moment is in parallel to the absorbing one)

$$F(\alpha, \varepsilon) = \frac{\Phi_F}{5n^2} * \{3 + \cos^2(\alpha_i + \varepsilon_i)\} \quad (3)$$

where  $n$  is the refractive index of the film, and  $F(\alpha, \varepsilon)$  is normalized to  $A(\alpha_0)$ .

In the evaporated films the  $n$ T molecules are preferentially oriented with their long axes in parallel to the normal of the film. Perfect alignment in this direction yields

$$F(\varepsilon) = \frac{\Phi_F}{n^2} * \sin^2 \varepsilon_i \quad (4)$$

i.e., a very different angular distribution of the fluorescence intensity. The experimental tilt angle of  $\Theta = 15^\circ$ , found for ultrathin 5T films, reduces this difference as well as further disorder in the thicker films and fluorescence depolarization by intermolecular energy transfer.

We considered Eqs. (3) and (4) in the calculation of  $\Phi_F$ , but because of the uncertainties in molecular orientation, anisotropic refractive index, energy transfer, surface roughness, etc., we were not able to reduce the error bar to less than ca. +100 and –50%. However, this error bar is still small enough to classify significantly the condensed  $n$ T phases with respect to their fluorescence quantum yields.

## RESULTS AND DISCUSSION

### Fluorescence Yields

Table I presents a selection of data that are typical for condensed  $n$ T phases inclusive of the small (5T) $_x$  clusters. In all cases the fluorescence yields are distinctly lowered compared to the single molecules in solution. The yields are especially low in ultrathin films, where the molecules are highly oriented with their long axes in parallel to the normal of the substrate surface [25]. This orientation is found to be very strong from 5T to 8T but only weak for 3T and 4T. Correspondingly higher are the yields of the latter “films” (in reality, 3T and 4T form crystalline islands at low surface loadings). With increasing film thickness the molecules lose more and more their preferential orientation with respect to the substrate, and the fluorescence yields increase by ca. one order of magnitude. Upon cooling to 77 K the fluorescence intensities increase by an additional factor of three to five. The yields, however, are still significantly lower than in dilute solution (the exception may be thin 4T films, whose low temperature yields approach about 50% of the room-temperature value in solution).

### Absorption and Fluorescence Spectra

Absorption spectra vary systematically with the chain length, layer thickness, deposition rate, and substrate temperature and, to some extent, also with the nature of the substrate. Here only the general features of the spectra are described as far as they will help to understand the deactivation processes.

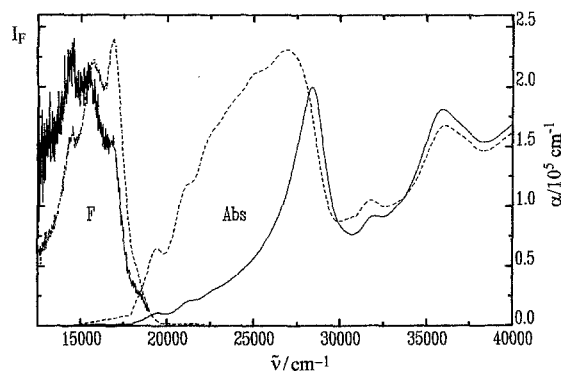


Fig. 3. Absorption spectra (scaled to the absorption coefficient per unit length of the layer thickness) and fluorescence spectra of 6T films with  $d = 10$  nm (solid lines) and  $d = 30$  nm (dashed lines) recorded under  $\alpha_0 = 60^\circ$ .

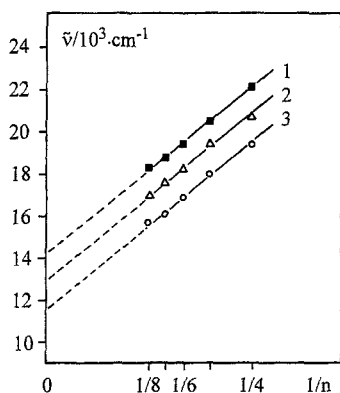


Fig. 4. Electronic transition energies of oligothiophenes  $nT$  in thin VD films vs reciprocal ring number  $1/n$ . (1) First absorption peak; (2) fluorescence shoulder; (3) first fluorescence maximum.

In solution or dissolved in polymer matrices the fluorescence and first allowed absorption band are assigned to the  ${}^1A_g \leftrightarrow {}^1B_u$  (HOMO  $\leftrightarrow$  LUMO) transition. In ultrathin VD films of 5T–8T the absorption maximum of this transition shifts considerably to the blue (see Fig. 2, middle) in a similar way as found in Langmuir–Blodgett films [16,17,19], but quantitatively even stronger. The blue shift is explained by a collective in-phase excitation of a large ensemble of the film constituting units, according to the molecular exciton model. In the extreme case of an infinitely extended two-dimensional layer with oscillators in parallel to the surface normal, only the transition with  $k = 0$  is allowed, i.e., the transition to the highest energy level of the exciton band (H aggregates). In reality this sharp selection rule is broken up, because the layer is not infinite, the oscillators are not exactly in parallel, and the wavelength of irradiation

is short, so that adjacent oscillators are excited with a phase difference of  $0.5^\circ$ . As a consequence, the  ${}^1B_u$ -exciton absorption band tails widely to the red with the origin somewhere at  $\leq 18,000$   $\text{cm}^{-1}$  (6T) or  $\geq 19,000$   $\text{cm}^{-1}$  (5T), and drops steeply at the blue side of the maximum (see Figs. 2 and 3). Increasing film thickness reduces the long range molecular order and breaks up the  $k = 0$  selection rule even more. As a result the red tail of the exciton band gains intensity, as can be clearly seen in Fig. 3 for 6T (not so clearly for 5T, because this film retains long-range orientation up to  $d \approx 30$  nm).

Close to the origin of the  ${}^1B_u$ -exciton absorption band, an additional series of weak absorption peaks is located that shift systematically to the red with the ring number of  $nT$ . The absorption coefficients of these peaks increase with the layer thickness from  $\alpha \approx 1 \cdot 10^4$   $\text{cm}^{-1}$  for ultrathin layers to  $\alpha \approx 3 \cdot 10^4$   $\text{cm}^{-1}$  for the more disordered thicker layers (see, e.g., Fig. 3), and one could argue that these peaks are due to the  ${}^1B_u$ -absorption of disordered  $nT$  aggregates, i.e., to localized  ${}^1B_u$  excitons. However, recently the two-photon absorption spectrum of 6T films at  $T = 4.2$  K was published [21] that shows the structured transition to the first excited  $2^1A_g$  state. The region of this transition coincides exactly with the first peak in our 6T films, and we therefore assign this peak in 6T, and also in the other  $nT$  films, to the  $1^1A_g \leftrightarrow 2^1A_g$  transition. This transition is symmetry forbidden for one-photon absorption, but it gains intensity from the neighboring  $B_u$  transition the closer these two transitions are located (the situation is similar to 1,6-diphenylhexatriene [26]). Thus the red shift of the  ${}^1B_u$  absorption with the layer thickness can also explain the increase in the absorption coefficient of the  $2^1A_g$  peak.

According to the band assignments, the fluorescence spectra of the  $nT$  films originate either from a low-lying  ${}^1B_u$  exciton state or from  $2^1A_g$ . Both transitions are forbidden. The fluorescence of the ultrathin layers is broad, almost unstructured, and very weak so that it is impossible for the moment to exactly localize its origin. However, the fluorescence subpeaks of the thicker films clearly correlate with the position of the first  $2^1A_g$  absorption peak. All fluorescence spectra have in common a weak high energetic shoulder or peak and then an equidistant series of two or three intense maxima and additional shoulders in the red (the low-temperature spectrum of 4T shows two of such series). As illustrated in Fig. 4 the peak positions give parallel straight lines when plotted over  $1/n$ , the reciprocal ring number of the thiophenes. Of course, this is no proof that the fluorescence must arise from  $2^1A_g$ , but since the fluorescence excitation spectra show no indication of an additional

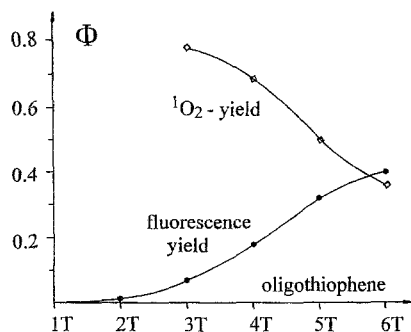


Fig. 5. Absolute fluorescence quantum yields and  $^1\text{O}_2$  quantum yields of oligothiophenes in dichloromethane and benzene, respectively. The concentrations were adjusted to equal absorbances of 0.05 at the excitation wavelength. The  $^1\text{O}_2$  quantum yields are given relative to phenazine ( $\Phi_\Delta = 0.88$ ).

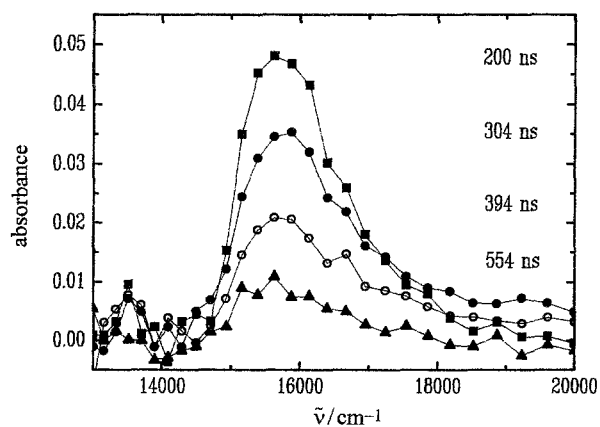


Fig. 6. Time-resolved triplet-triplet absorption spectra of 5T in dioxane ( $c = 1 \times 10^{-5} M$ ), saturated with air. First-order decay time  $\tau = 0.24 \mu\text{s}$ . Under nitrogen the decay time rises to  $\tau = 7.75 \mu\text{s}$ . Excitation at  $\lambda^a = 354 \text{ nm}$  with a Nd/YAG laser pulse of 23 mJ.

absorption band below  $2^1A_g$ , it is not necessary for the moment to assume that  $2^1A_g$  is not the emitting state.

### Nonradiative Deactivation

The main part of the excited thiophenes deactivate by nonradiative processes, even in solution. The usual deactivation pathway for dissolved poly- $\pi$ -conjugated molecules is that via triplet states. Unfortunately no unambiguous evidence of  $nT$  phosphorescence was given up to now, but the triplet pathway was proven for 2T and 3T by the triplet-triplet absorption (TTA) spectra [3,5,6] and indirectly by the production of singlet oxygen,  $T_1 + ^3\text{O}_2 \rightarrow S_0 + ^1\text{O}_2$  (the reaction of thiophenes in the excited singlet state,  $S_1 + ^3\text{O}_2 \rightarrow T_1 + ^1\text{O}_2$ , is of minor importance because of the very short  $S_1$  lifetimes).

We determined the  $^1\text{O}_2$  yields,  $\Phi_\Delta$ , for all soluble thiophenes and found a clear complementary correlation to the fluorescence yields (see Fig. 5). The high value of the sum  $\Phi_F + \Phi_\Delta \geq 0.8$  also shows clearly that fluorescence and triplet formation are by far the most predominant deactivation processes of excited  $nT$ 's in solution. In addition, the TTA of dissolved  $nT$  can easily be measured and kinetically analyzed, even in oxygen-containing solution. An example is given in Fig. 6.

We carried out the same experiment for small clusters ( $5T$ )<sub>5-8</sub>, dissolved in a 1:1 dioxane/ $D_2O$  mixture (for spectra see Fig. 2, bottom), and found not a trace of  $^1\text{O}_2$  production and, also, not a trace of TTA (in the latter case the solution was free of oxygen). Thus the triplet formation yield in 5T aggregates (and very probably also in the film) must be by orders of magnitude lower than in the single molecule. Since also fluorescence is a negligible deactivation step, the main pathways must be either internal conversion, ( $S_1S_0^* \rightarrow S_0S_0^* + E_{\text{vib}}$ ) or sudden polarization ( $^1(S_1S_0^*) \rightarrow ^1(D^+D^{*-})$ ). The doublets either recombine to the ground state, but not via  $^3(D^+D^{*-})$ , or have a certain probability to dissociate like in exciplexes to ( $^2D^{*+}D^{*-}$ ) and to lose their spin correlation. The consequence of the latter process is photoconductivity.

### ACKNOWLEDGMENTS

The oligothiophenes were kindly supplied by H. Naarmann, BASF AG, Ludwigshafen, Germany. This work was financially supported by the BMFT (TK0323/0) and by the DAAD (ARC program).

### REFERENCES

1. R. Eckert, H. Kuhn (1960) *Z. Elektrochem.* **64**, 357.
2. B. Norden, R. Hakansson, and M. Sundbom (1972) *Acta Chem. Scand.* **26**, 429.
3. J. P. Reyftmann, J. Kagan, R. Santus, and P. Morliere (1985) *Photochem. Photobiol.* **41**, 1.
4. R. H. Abu-Eittah and F. A. Al-Sugeir (1985) *Bull. Chem. Soc. Jpn.* **58**, 2126.
5. J. C. Scaiano, A. MacEachern, J. T. Arnason, P. Morand, and D. Weir (1987) *Photochem. Photobiol.* **46**, 193.
6. J. C. Scaiano, C. Evans, and J. T. Arnason (1989) *J. Photochem. Photobiol.* **B3**, 411.
7. C. V. Pham, A. Burckhardt, R. Shabana, D. D. Cunningham, H. B. Mark, and H. Zimmer (1989) *Phosphorus Sulfur Silicon* **46**, 153.
8. D. Birnbaum and B. E. Kohler (1989) *J. Chem. Phys.* **90**, 3506.
9. J. Guay, P. Kasai, A. Diaz, R. Wu, J. M. Tour, and L. H. Dao (1992) *Chem. Mater.* **4**, 1097.
10. P. Bäuerle (1992) *Adv. Mat.* **4**, 102.
11. D. Birnbaum, D. Fichou, and B. E. Kohler (1992) *J. Chem. Phys.* **96**, 165.

12. H. Chosrovian, D. Grebner, S. Rentsch, and N. Naarmann (1992) *Synth. Met.* **52**, 213.
13. H.-J. Egelhaaf, P. Bäuerle, K. Rauer, V. Hoffmann, and D. Oelkrug (1993) *J. Mol. Struct.* **293**, 249.
14. S. L. Bondarev, I. I. Ivanov, Yu. N. Romashin, and O. G. Kulinovich (1992) *J. Appl. Spectrosc.* **56**, 440.
15. H. Chosrovian, S. Rentsch, D. Grebner, D. U. Dahm, E. Birckner, and H. Naarmann (1993) *Synth. Met.* **60**, 29.
16. U. Schoeler, K. H. Tews, and H. Kuhn (1974) *J. Chem. Phys.* **61**, 5009.
17. H. Nakahara, J. Nakayama, M. Hoshino, and K. Fukuda (1988) *Thin Solid Films* **160**, 87.
18. D. Fichou, G. Horowitz, B. Xu, and F. Garnier (1989) in H. Kuzmany, M. Mehring, and S. Roth (Eds.), *Electronic Properties of Conjugated Polymers III*, Springer Ser. Sol. State Phys., Vol. 91, Springer Verlag, Berlin, p. 386.
19. E. Vuorimaa, P. Yli-Lahti, M. Ikonen, and H. Lemmetyinen (1990) *Thin Solid Films* **190**, 175.
20. R. Lazzaroni, A. J. Pal, S. Rossini, G. Ruani, R. Zamboni, and C. Taliani (1991) *Synth. Met.* **41-43**, 2359.
21. R. Zamboni, N. Periasamy, G. Ruani, and C. Taliani (1993) *Synth. Met.* **54**, 57.
22. J. Shinar, Z. Vardeny, E. Ehrenfreund, and O. Brafman (1987) *Synth. Met.* **18**, 199.
23. J. L. Sauvajol, D. Chenouni, J. P. Lère-Porte, C. Chorro, B. Moukala, and J. Petrissans (1990) *Synth. Met.* **38**, 1.
24. F. Geiger, M. Stoldt, H. Schweizer, P. Bäuerle, and E. Umbach (1993) *Adv. Mat.* **5**, 992.
25. H.-J. Egelhaaf, P. Bäuerle, K. Rauer, V. Hoffmann, and D. Oelkrug (1994) *Synth. Met.* **61**, 143.
26. E. D. Cehelnik, R. B. Cundall, J. R. Lockwood, and T. F. Palmer (1975) *J. Phys. Chem.* **79**, 1369.